A Review of High Dynamic Range Front-End Amplifiers

by

Chris Trask / N7ZWY
Sonoran Radio Research
P.O. Box 25240
Tempe, AZ 85285-5240

Email: christrask@earthlink.net

25 July 2015

Introduction

Designers of small-signal amplifiers, whether they be for telecommunications, radio astronomy, medical instrumentation, or audio, are forever faced with the problem of excess noise, often referred to as noise figure or noise temperature. Methods for decreasing the low-frequency components of this excess noise, known as 1/f or shot noise, have been successfully addressed, however it has only been in recent years that high frequency noise components, known as thermal or flicker noise, have been dealt with.

In this paper, some popular methods for suppressing high frequency circuit noise in monolithic amplifiers will be reviewed, and alternative methods having wider application and suitable for realizations using discrete components will be proposed and examined. Both methods are also useful in the reduction of intermodulation distortion (IMD) products.

A Brief Overview of Semiconductor Device Noise

Before getting involved with details of circuitry, it is necessary that we gain a minimal understanding of the nature of noise in solid state circuitry. The primary types of noise encountered are 1/f, also known as shot noise, and thermal, also known as flicker noise. This latter form of noise is generally wideband and of even spectral distribution, whereas the former is concentrated at lower frequencies, as its name suggests, and its spectral distrubution is inversely logarithmic, as is shown for a typical 2N4957 bipolar transistor in Fig. 1 (1). Both forms of noise are to be found in virtually all semiconductor devices, thermal noise being due primariy to bulk resistances in the semiconductor material while 1/f noise in bipolar transistors is due primarily to the fluctuation in the recombination rate of charge carriers in the emitter junction depletion layer (2). These noise sources are highly dependent on factors such
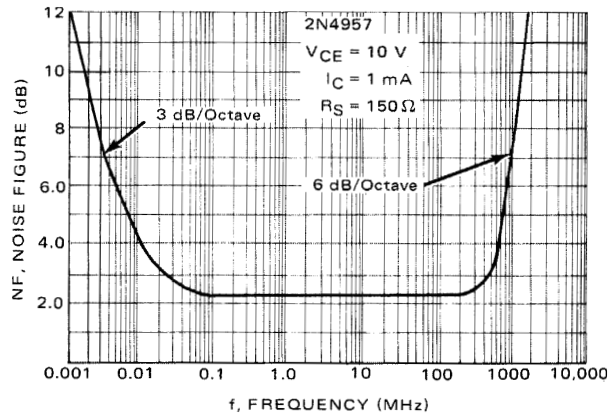

Figure 1 - Shot Noise Figure for a Typical Bipolar Transistor

as the collector (or drain) bias current (I_C), the collector-emitter (or drain-source) bias voltage (V_{CE}), and the source resistance (R_S) (3). Fig. 2 illustrates these dependencies for a typical 2N4401 bipolar transistor.

Cancelling 1/f Noise

The cancellation of 1/f noise has been reduced to practice in the design of both oscillators and lossless feedback (aka Norton) amplifiers by methods that are roughly similar.

In oscillators, 1/f noise generated by the oscillator transistor is detected, amplified, and
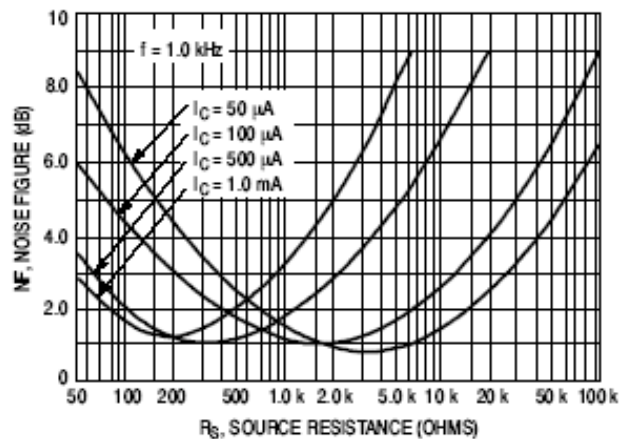

Figure 2 - Wideband Noise Figure for a Typical Bipolar Transistor with Respect to Source Resistance and Collector Current

inverted by a low-frequency low-noise device and then applied to the input of the oscillator device, forming a closed negative feedback loop, the result being that the lower 1/f noise of the low-frequency transistor dominates (4,5). This serves to greatly decrease the single-sideband (SSB) phase noise of the oscillator, which is a serious problem in microwave frequency sources.

In lossless feedback amplifiers, 1/f noise at the emitter of the amplifier device is detected, amplified, and inverted by a low-frequency low-noise device and then applied to the base of the amplifier device, again forming a closed negative feedback loop in which the lower 1/f noise of the low-frequency transistor dominates (6, 7). In amplifiers as well as active mixers, the 1/f noise modulates the bias current and in turn modulates the signal, creating both AM and FM noise that has the same baseband spectral characteristics to either side of the signal (2, 8, 9).

Both methods are similar in concept to the method of active feedback proposed by Walls *et al* (8) and have been proven to be effective in the suppression of 1/f noise, however none of these methods are capable of reducing the effects of thermal noise.

The Bruccoleri Thermal Noise Canceling Amplifier

An interesting innovation in small-signal amplifier design was proposed in 2002 by Bruccoleri *et al* of the University of Twente that cancels both thermal noise and IMD products (10, 11, 12, 13). Shown in it's basic form in Fig. 3, the Bruccoleri amplifier consists of a pair of amplifiers and a feedback resistor. The first amplifier A_1 output has the amplified input signal as well as the IMD products and noise of the transistor, and the output signal is in opposite phase of the input signal. At the junction of the two resistors and the transistor gate, there is a small amount of signal that is of opposite
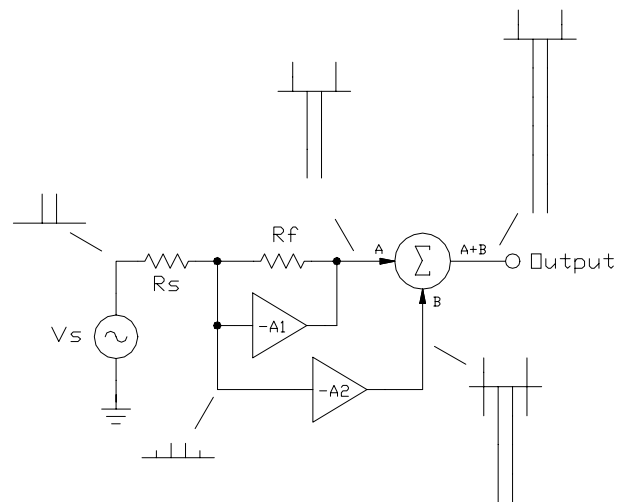

Figure 3 - Concept of Bruccoleri's Thermal Noise Canceling Amplifier (adapted from reference 10)

phase to the output signal and an equally small amount of the IMD products and output noise that is in phase with the output IMD products and noise. Amplifier A_2 then amplifies the junction signal so that its output has the IMD products and noise of the output of the feedback amplifier and which is of equal amplitude and opposite phase together with an amplified input signal that has the same phase and amplitude as the feedback amplifier. These two output signals are then summed, resulting in a doubling of the output signal and a reduction of the feedback amplifier IMD products and noise.

Unfortunately, the circuit is not capable of simultaneous noise and IMD cancellation, and further it is not capable of simultaneously canceling third-order (IM_3) and second-order (IM_2) products (10). Further, in the analysis of Fig. 3 amplifier A_2 is considered to be both noise-and-distortion-free, Notwithstanding, a reasonable approximation to simultaneous cancellation is however achievable in practice. Despite these and other minor shortcomings, the circuit has gained some degree of popularity amongst designers of wideband amplifiers for television and telecommunications receivers (14, 15, 16, 17).
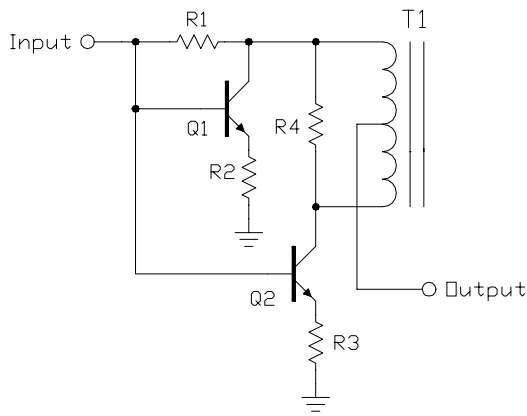
Figure 5 - Discrete Realization of Bruccoleri's
Thermal Noise Cancelling Amplifier

The Discrete Bruccoleri Thermal Noise Canceling Amplifier

As shown in Fig. 5, the Bruccoleri amplifier can be realised in discrete form. Here, transistor Q_1 and resistors R_1 and R_2 comprise the negative feedback amplifier A_1 of Fig. 3, while transistor Q_2 and resistor R_3 comprise amplifier A_2 of Fig. 3. The power splitter/combiner consisting of transformer T_1 and resistor R4 comprise the summation function of Fig. 3. If the two transistors have similar characteristics and biasing, the amplifier has twice the signal gain of the negative feedback amplifier alone, while the output noise and IMD products remain the same, potentially giving the amplifier a 6dB advantage in dynamic range.

Considerable experimentation with this circuit proved to be disappointing, though the 3dB improvement in OIP_3 performance was realised.

The Chin-Fu Signal Nulled Feedback Amplifier

An interesting furtherance of the Bruccoleri amplifier was proposed by Chin-Fu *et al* in 2008 (18). Shown in its basic form in Fig. 6, the Chin-Fu amplifier retains the feedback topology of Bruccoleri's first amplifier A_1, but then modifies the second amplifier A_2 so that just the noise and IMD products of ampli-
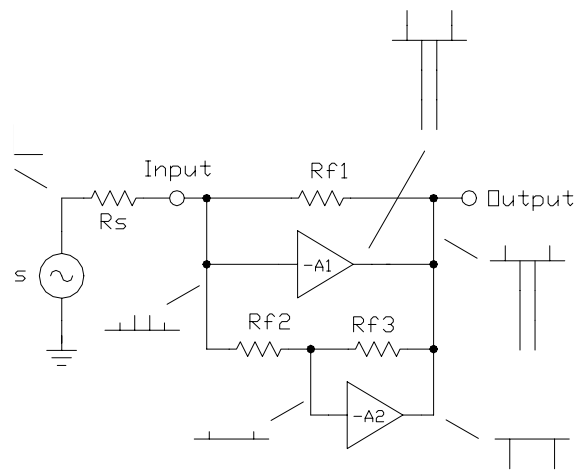

Figure 6 - Concept of the Chin-Fu
Signal Nulled Feedback Amplifier
(adapted from reference 18)

fier A1 are amplified by amplifier A_2.

The method is quite simple in concept and is as follows: Since the phase of the output signal is opposite that of the input signal, there exists a point along R_{FB} in Fig. 3 where there is a virtual signal null. At the same time, the output noise and IMD products of amplifier A_1 are not cancelled at this point, as shown in Fig. 6, where a voltage divider consisting of the two resistors R_{f2} and R_{f3} provides the desired signal nulling. Amplifier A_2 amplifies and inverts the scaled noise and IMD products, then sums it at the output to provided the desired cancellation, the degree of which improves as the signal gain of amplifier A_2 is increased

. A simplified version of the Chin-Fu amplifier is shown in Fig. 7, where the feedback resistor R_{f1} has been removed. The resistors R_{f2} and R_{f3} now serve as both the feedback
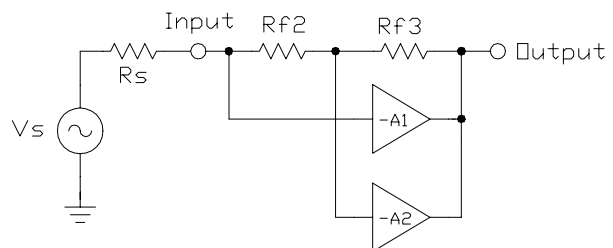

Figure 7 - Simplified Version of the
Chin-FuSignal Nulled Feedback Amplifier

path for amplifier A_1 as well as the voltage divider for amplifier A_2 and the sum of their values is equal to the value of the removed resistor R_{f1}.

The Series/Shunt Feedback Amplifier

The Bruccoleri and Chin-Fu amplifiers are certainly sources of inspiration for alternative approaches to the cancellation of thermal noise and IMD products. One such alternative can be realized by initially considering the series/shunt feedback amplifier, shown in Fig. 8. Patented in 1970 (19), this topology has improved distortion characteristics over the negative feedback amplifier employed by Bruccoleri and Chin-Fu as it incorporates two negative feedback loops, the advantage being due to the fact that linearity in general improves as the number of feedback loops is increased (20, 21, 22). The value of the shunt feedback resistor R_{FB} is determined by:

$$R_{FB} = R_S \left(1 + A_V\right) \tag{1}$$

where R_S is the source resistance and A_V is the amplifier voltage gain. The value of the series feedback resistor R_E is determined by:

$$R_E = \frac{1}{A_V}\left(\frac{R_L \, A_V \, R_S}{R_L + A_V \, R_S}\right) \tag{2}$$

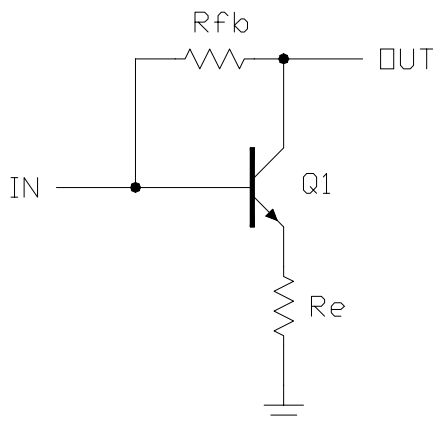where R_L is the load resistance. If R_L and R_S

Figure 8 - The Series/Shunt Feedback Amplifier

are identical, Eq. 2 reduces to:

$$R_E = \frac{R_L{}^2}{R_{FB}} \tag{3}$$

which then needs to be adjusted so as to incorporate the finite emitter resistance r_e of the transistor:

$$R'_E = R_E - r_E \tag{4}$$

$$r_E \approx \frac{r_{bb}}{h_{fe}} + \frac{k\,T}{q\,|I_C|} \tag{5}$$

where r_{bb} is the base spreading resistance of the transistor, Ic is the collector current, q is 1.60218×10^{-19}, k is Boltzman's constant (1.38066×10^{-23}), and T is the absolute temperature (298.16^0 K).

Referring now to Fig. 9, we now observe the IMD characteristics of the amplifier. Since the bulk of the distortion is a result of the nonlinearities of the base-emitter junction of the transistor, the IMD products also appear at the transistor emitter, and then appear amplified and inverted at the collector. The shunt feedback resistor Rfb of Fig. 8 has been divided into two resistors R_{FB1} and R_{FB2}, the values of which are determined by:

$$R_{FB1} = R_S \tag{6}$$

$$R_{FB2} = A_V \, R_S \tag{7}$$

so as to produce a virtual signal ground at their junction so that the signal is nulled and a scaled version of the noise and IMD products are now present. This is most convenient as we can now detect and measure the transistor noise and IMD products without any signal present.

The Discrete Chin-Fu Signal Nulled Feedback Amplifier

Applying the modified series/shunt amplifier of Fig. 9 to the modified Chin-Fu amplifier of Fig. 7 results in the convenient and elegant topology of Fig. 9 where amplifier A1 of Fig. 7
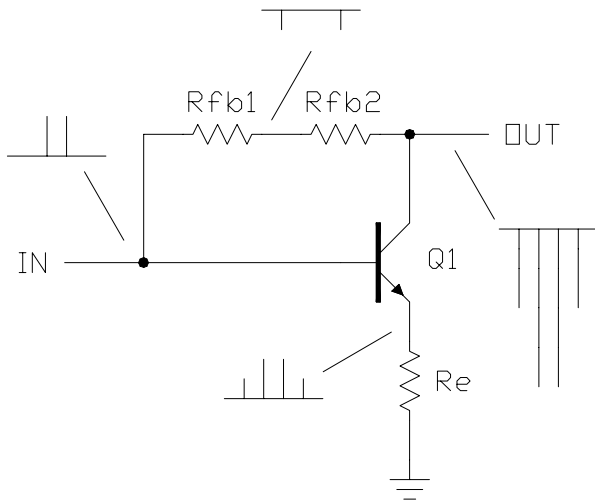
Figure 9 - Distortion Products in the
Series/Shunt Feedback Amplifier

consists of transistor Q_1 and resistor Re and amplifier A_2 of Fig. 7 consists of the common-emitter amplifier Q2 , whence will be referred to as the noise/error amplifier.

When considering the noise/error amplifier as being noiseless, as the gain of Q_2 is increased, the noise and IMD products seen at the input to the noise/error amplifier, being the junction of R_{FB1} and R_{FB2}, will diminish to zero as the gain approaches infinity. This in turn results in no noise or IMD products at the amplifier output.
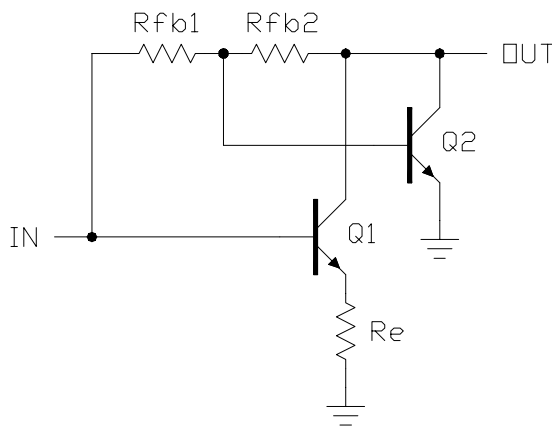
With regard to practical realization, for fi-

Figure 9 - Discreate Realisation of the
Simplified Chin-Fu Signal-Nulled
Feedback Amplifier

nite values of gain for Q_2 there will remain some small amount of noise and IMD products from signal amplifier transistor Q_1 appearing at the output which will be added the noise of the noise/error amplifier transistor Q_2.

At the same time, owing to the lack of desired signal at the base of Q_2, the amount of IMD products generated by the noise/error amplifier will be insignificant. Consequently, the dynamic range requirements for Q_2 are greatly diminished, which which results in a significant degree of flexibility in the overall design. Returning to the earlier discussion about the dependency of NF on biasing conditions, transistor Q_2 can be operated at an appreciably lower bias current where it has a more favourable NF, while still having sufficient dynamic range to accomodate the low levels of noise and IMD products from signal amplifier transistor Q_1.

Prototype Design and Evaluation

A protype push-pull amplifier using a pair of simplified Chin-Fu amplifiers having 12dB of gain was constructed and evaluated, the schematic of which is shown in Fig. 10. Using Eq. 6, the value for resistors R_4 and R_6 is:

$$R_4 = R_6 = 2 N^2 R_S \qquad (8)$$

where N is the turns ratio of the 1:N:N transformers T_1 and T_2. Using Eq. 7, the value for resistors R_5 and R_7 is determined by:

$$R_5 = R_7 = 2 N^2 R_S A_V \qquad (9)$$

Using Eq. 3, Eq. 4, Eq. 8, and Eq. 9, the emitter resistor R'_E required is:

$$R'_E = \frac{1}{A_V}\left(\frac{\left(2 N^2 R_L\right)R_5}{2 N^2 R_L + R_5}\right) - r_e =$$

$$= \frac{1}{A_V}\left(\frac{R_5 R_4}{R_5 + R_4}\right) - r_e \Bigg|_{R_S = R_L} \qquad (10)$$

where r_E is the emitter resistance, determined by Eq. 5. The resistor network consisting of

C1, C2, C3, C4, C5 - 0.1uF   R1, R2, R3 - 51 ohms
C6 - 47uF 16WVDC   R4, R6 - 100 ohms
                                    R5, R7 - 390 ohms
D1 - 1N4148   R8, R9 - see text
                                    R10 - see text
                                    R11 - 220 ohms
Q1, Q2 - 2N2222
Q3, Q4 - See text

                                    T1, T2 - 1:2CT (Mini-Circuits
                                        T4-1 or T4-6T)

Figure 10 - 12dB Simplified Li Amplifier Schematic and Parts List

R_1, R_2, and R_3 is convenient as it allows for the use of encapsulated resistor network SIPs that track far better over temperature than do individual resistors, and the value for R_1, R_2, and R_3 is determined by:

$$R_1 = R_2 = R_3 = 3R'_E \qquad (11)$$

Resistor R_{10} is selected to produce the desired collector current for the signal amplifier transistors Q_1 and Q_2, while resistors R_8 and R_9 are selected to produce the desired collector current for the noise/error amplifier transistors Q_3 and Q_4.

A considerable amount of testing was done with this circuit at a frequency of 10MHz, exploring various collector currents for Q_1/Q_2 and Q_3/Q_4. In the end, a collector current of 10mA for Q_1/Q_2 was found to give the best combined performances for NF and IMD, and the collector current for Q_3/Q_4 was varied over a range to provide a performance range suitable for demonstrating the performance that can be attained, which is shown in Fig. 11. Note that there is a fairly decent improvement in NF for a Q_3/Q_4 collector current of 150mA, but there is little improvement in IMD performance even with a Q_3/Q_4 collector current of 1mA. This may be due to the NF of Q_3/Q_4 deteriorating with
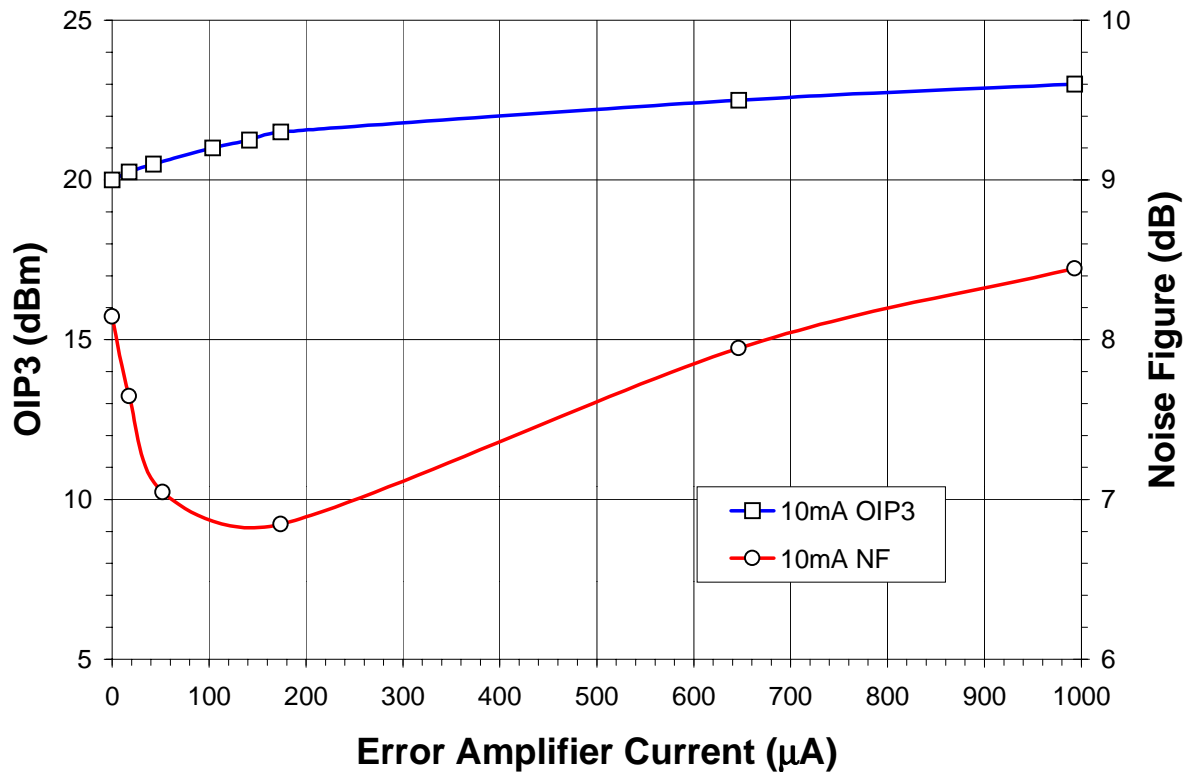
Figure 11 - IMD and Noise Figure Performance vs. Error Amplifier Current

increased collector current, resulting in masking the closed-loop NF improvement of Q1/Q2. Though a bit disappointing with regard to the lack of appreciable improvement in IMD performance, the NF results show that there is some value to this topology, and further investigation with different transistors may prove worthwhile.

The Augmented Series/Shunt Feedback Amplifier

The supposition that noise from Q_3/Q_4 in the simplified Chin-Fu amplifier is impacting the overall NF of the amplifier begs the question if a similar amplifier can be devised that does not require an active noise/error amplification stage. One such possibility is shown in Fig. 12, where the error/noise signal at the virtual signal ground at the junction of R_{fb1} and R_{fb2} is coupled to the base of of the amplifier transistor Q_1 by way of a signal combiner, thus augmenting the amplifier by providing an additional

feedback loop that consists of just the inverted and scaled IMD products and noise of Q_1. Initially this would be considered to be impractical as the input ports of the signal combiner should be isolated. However, an approximation can be made by realising that the signal input port and the virtual signal ground are both of relatively low impedance while the base of Q_1 is of relatively high impedance. Initial
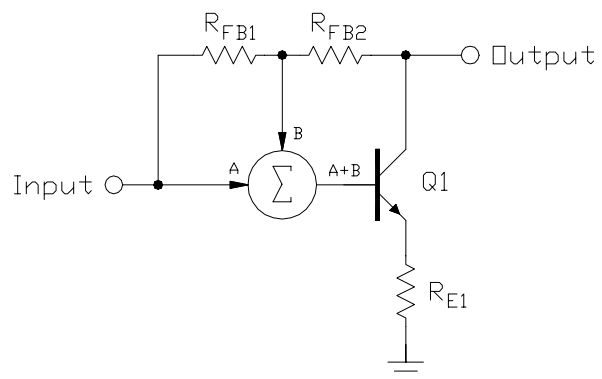

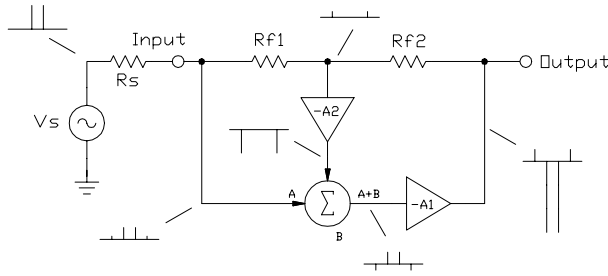Figure 12 - Generalised Schematic of the Augmented Series/Shunt Amplifier

Figure 13 - Generalised Distortion Model
of the Augmented Series/Shunt Amplifier

Figure 14 - Generalised Schematic of
the Augmented Series/Shunt Amplifier
with Passive Feedback

PSpice simulations shows this approximation to be valid. Interestingly, transistor Q_1 is providing its own predistortion.

Referring to Fig. 13, the distortion model of the augmented series/shunt amplifier includes a distortion-free amplification stage of voltage gain B between the signal null and the signal combiner. The open-loop distortion voltage seen at the output is determined by way of:

$$V_{OUT} = -\left(\frac{A\,V_{OUT}\,R_S}{R_S + R_{F1} + R_{F2}}\right) -$$
$$-\left(\frac{A\,B\,V_{OUT}\,(R_S + R_{F1})}{R_S + R_{F1} + R_{F2}}\right) + V_{IMD} \quad (12)$$

where V_{IMD} is the open-loop distortion voltage and A is the voltage gain of the amplifier. Eq. 13 is the closed-form solution, which shows that the output distortion decreases as the error/ noise signal gain B increases, and becomes zero as B approaches infinity:

$$V_{OUT} \to 0\big|_{B\to\infty} \quad (14)$$

A passive realisation of the augmented series/shunt amplifier is shown in Fig. 14, where a wideband transformer of turns ratio N:1 is used as the signal combiner. The resulting output distortion voltage is approximately that of Eq. 13, substituting N for the error/noise gain variable B, as shown in Eq. 15.

Referring to Fig. 15, the noise model of the augmented series/shunt amplifier includes the input noise sources V_N of amplifier A. The open-loop equation for the total output noise is:

$$V_{OUT} = -\left(\frac{A\,V_N\,R_S}{R_S + R_{F1} + R_{F2}}\right) -$$
$$-\left(\frac{A\,B\,V_N\,(R_S + R_{F1})}{R_S + R_{F1} + R_{F2}}\right) - A\,V_N \quad (16)$$

and Eq. 17 is the closed-loop form. In the same manner as with the discussion of the distortion properties, when the signal gain B is increased to infinity, the total output noise becomes:

$$V_{OUT} \to 0\big|_{B\to\infty} \quad (18)$$

$$V_{OUT} = V_{IMD}\left(\frac{R_S + R_{F1} + R_{F2}}{R_S\,(1 + A + AB) + R_{F1}\,(1 + AB) + R_{F2}}\right) \quad (13)$$

$$V_{OUT} \approx V_{IMD}\left(\frac{R_S + R_{F1} + R_{F2}}{R_S\,(1 + A + AN) + R_{F1}\,(1 + AN) + R_{F2}}\right) \quad (15)$$

$$V_{OUT} = -A\,V_N\left(\frac{R_S + R_{F1} + R_{F2}}{R_S\,(1 + A + AB) + R_{F1}\,(1 + AB) + R_{F2}}\right) \quad (17)$$
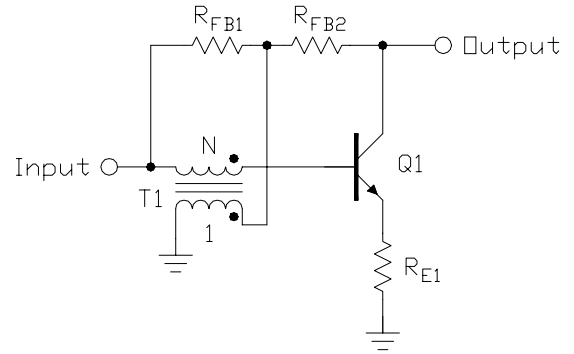
$$V_{OUT} = -A\,V_N \left(\frac{R_S + R_{F1} + R_{F2}}{R_S\,(1 + A + AN) + R_{F1}\,(1 + AN) + R_{F2}} \right) \qquad (19)$$

Referring back to Fig. 14, where a wideband transformer of turns ratio N:1 is used as the signal combiner, the resulting output noise voltage for a passive realisation of the augmented series/shunt amplifier is approximately that of Eq. 17, substituting N for the error/noise gain variable B, as shown in Eq. 19.

Prototype Design and Evaluation

The topology and analysis of the augmented series/shunt amplifier indicates that the noise and distortion performance of the common series/shunt amplifier can be improved by providing an additional feedback path that consists of a lossless, distortion-free wideband transformer. To evaluate the degree of improvement, a prototype circuit was constructed, the schematic of which is shown in Fig. 16. In order to make a proper comparison with the earlier simplified Chin-Fu amplifier of Fig. 10, the same parts were used, and the overall modifications consisted mainly of the inclusion of transformer T_2.

Some discussion of tranformer T_2 is necessary as it is not exactly straight-forward. Since the circuit is balanced rather than single-sided, the secondary winding is shared between the two sides. To be consistent with good wideband transformer construction practice, only those configurations that can be achieved
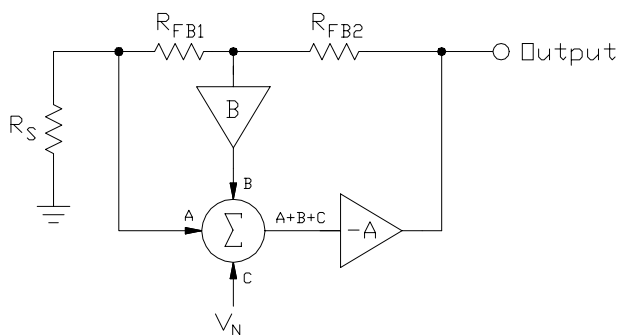
with 2-wire bifilar and 3-wire trifilar windings were used (23).

The first form was made with a single winding of three trifilar turns on a Fair-Rite 2843002402 binocular core, shown in Fig. 17. This results in a 1:1:1 transformer for the balanced amplifier, which is the equivalent of a 1:0.5 (or 2:1) transformer for a single-sided amplifier.

The second form was made with a pair of three bifilar turns on a Fair-Rite 2843002402 binocular core, with one wire from each bifilar pair connected in series, as shown in Fig. 18. This results in a 1:2:1 transformer for the balanced amplifier, which is the equivalent of a 1:1 transformer for a single-sided amplifier.

Lastly, a third form was made with a pair of trifilar turns on a Fair-Rite 2843002402 binocular core, with two wires from each trifilar bundle connected in series alternately, as shown in Fig. 19. This results in a 1:4:1 transformer for the balanced amplifier, which is the equivalent of a 1:2 transformer for a single-sided amplifier.

Testing conditions are kept as with the previous circuit shown in Fig. 10 so as to make a proper comparison, with R_{10} having been adjusted for the same 10mA of collector current for Q_1/Q_2. Both NF and IMD tests were performed at a frequency of 10MHz.
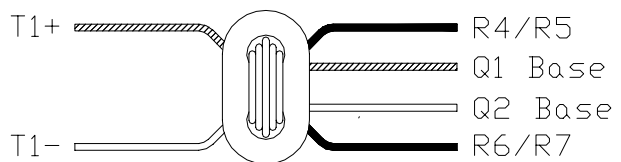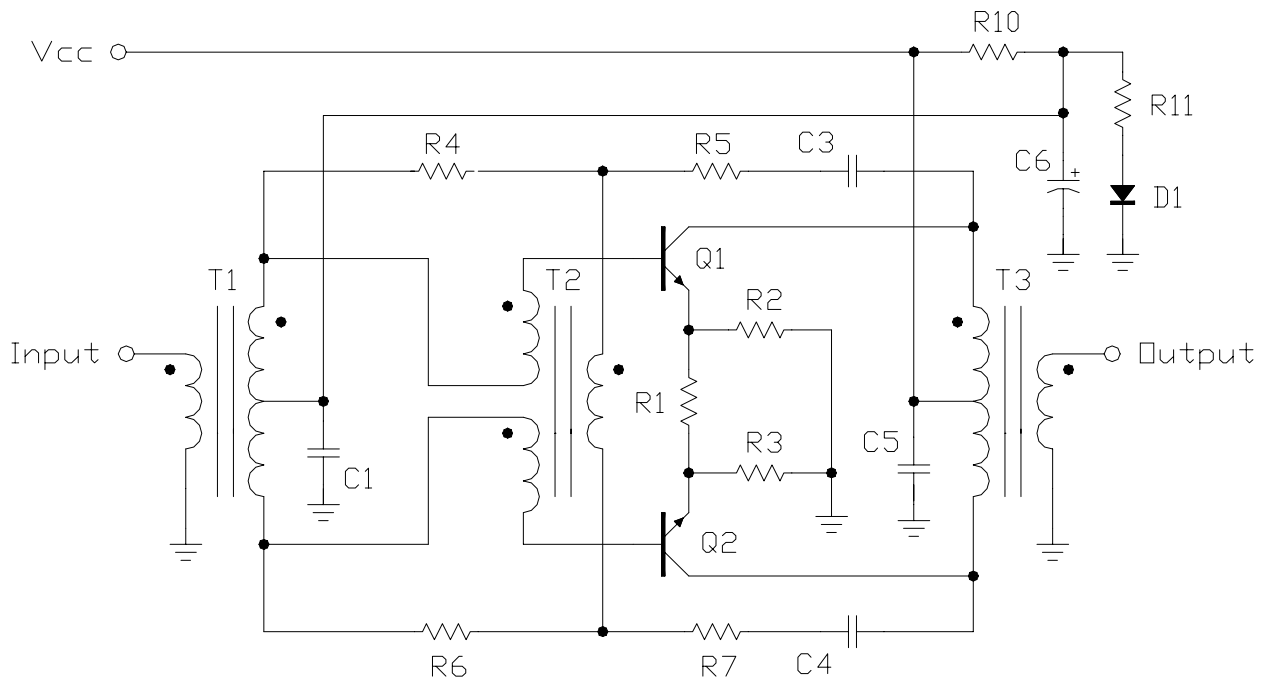

Figure 15 - Generalised Noise Model of the Augmented Series/Shunt Amplifier

Figure 17 - 1:1:1 Transformer T3 Details

C1, C3, C4, C5 - 0.1uF   R4, R6 - 100 ohms
C6 - 47uF 16WVDC   R5, R7 - 390 ohms
                                  R10 - see text
D1 - 1N4148   R11 - 220 ohms

Q1, Q2 - 2N2222   T1, T3 - 1:2CT (Mini-Circuits
                                      T4-1 or T4-6T)
R1, R2, R3 - 51 ohms   T2 - see text

Figure 16 - Balanced 12dB Augmented Series/Shunt Amplifier Schematic and Parts List

The test results given in Fig. 20 show that the augmented series/shunt amplifier has a significant advantage in IMD performance over the earlier modified Chin-Fu amplifier, and it appears that at least for the devices and transformers used, the improvement in OIP_3 is directly proportional with the turns ratio of transformer T_2.

The NF performance shows a moderate improvement over that of the modified Chin-Fu amplifier, but the minimum was unexpected. Simulations with PSpice verfied that this would occur with varying turns ratios of transformer T_2, and the hypothesis here is that the source impedance seen by the base of transistor Q_1 varies as the turns ratio N of T_2 is varied. Referring to Fig. 21, the source impedance R_N seen by the base of transistor Q_1 can be approximated as:
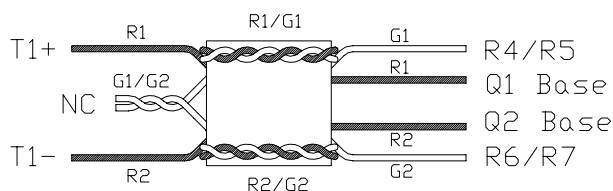

Figure 18 - 1:2:1 Transformer T3 Details

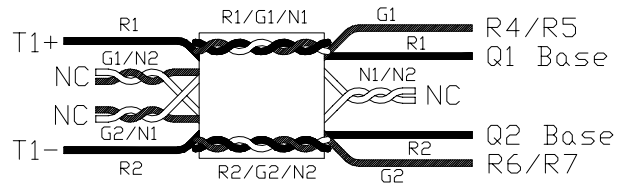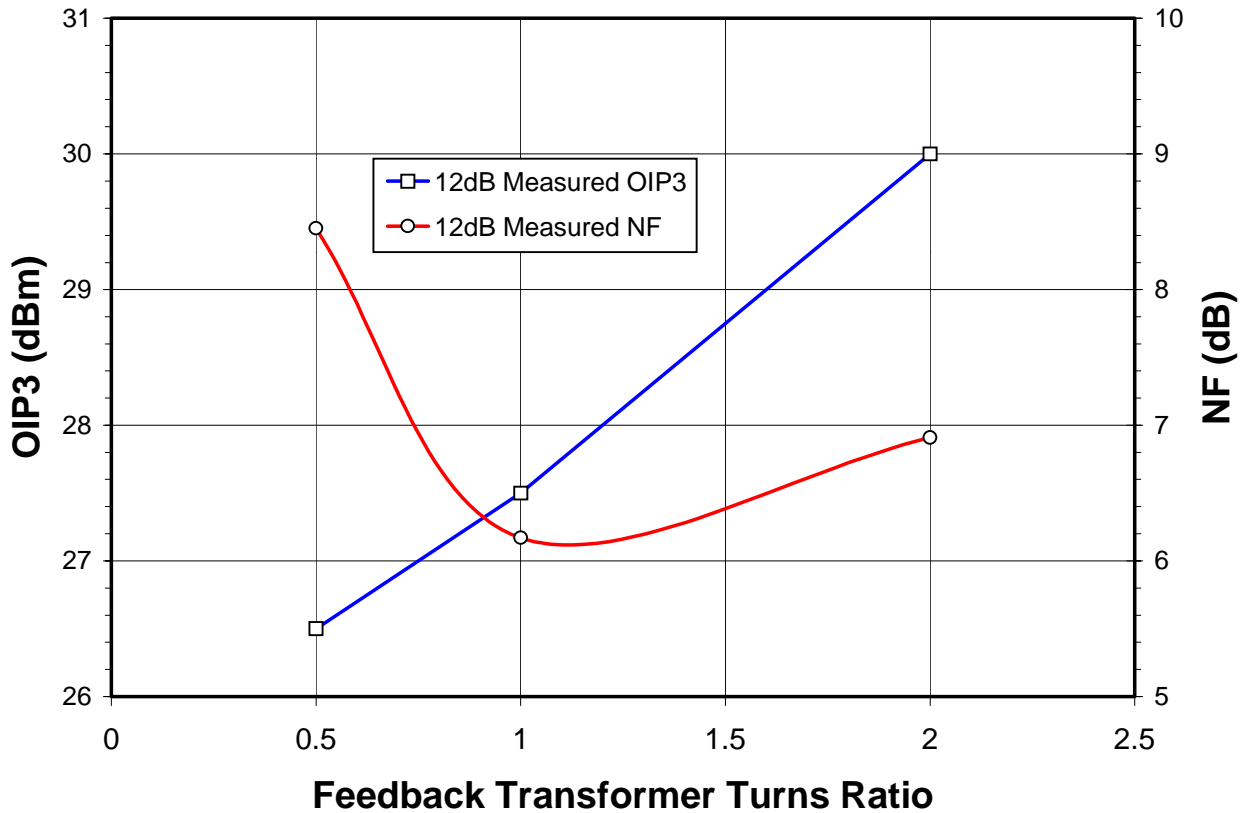Figure 19 - 1:4:1 Transformer T3 Details

Figure 10 - 12dB Proposed Amplifier IMD and NF Performance

$$R_N \approx R_S \parallel (R_{F1} + R_{F2} + R_L) +$$
$$+ N(R_S + R_{F1}) \parallel (R_{F2} + R_L) =$$
$$= \frac{R_S(R_{F1} + R_{F2} + R_L)}{R_S + R_{F1} + R_{F2} + R_L} +$$
$$+ \frac{N(R_S + R_{F1})(R_{F2} + R_L)}{R_S + R_{F1} + R_{F2} + R_L} \qquad (20)$$

This presents interesting possibilities, as the NF of the augmented series/shunt ampli-

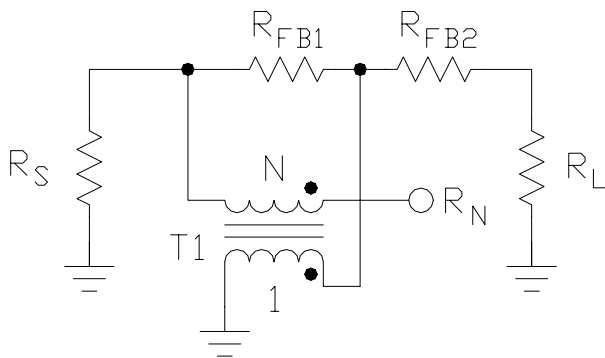
Figure 21 - Source Impedance Model of
the Augmented Series/Shunt Amplifier

fier can be adjusted by selecting an appropriate turns ratio N for transformer T_2, while at the same time transformer T_2 provides improved IMD performance over other forms of small signal amplifiers discussed here.

Synopsis

Various forms of amplifiers have been shown in the literature to provide improved NF performance by way of feedforward (Bruccoleri) and signal nulling (Chin-Fu *et al*) and other signal combining techniques (24). These amplifiers discussed herein have provided inspiration in devising yet another topology that provide improved NF and IMD performance and which can be reduced to practice using common discrete components.

References

1. Brubaker, R., *Semiconductor Noise Figure Considerations*, Motorola Application Note AN-421, August 1972.
2. Kuleshov, V.N. and T.I. Boldyreva, "1/f AM and PM Noise in Bipolar Transistor Amplifiers: Sources, Ways of Influence, Techniques of Reduction," 1997 IEEE International Frequency Control Symposium (IFCS 1997), pp. 446-455.
3. Cherry, E.M. and D.E. Hooper, "Amplifying Devices and Low-Pass Amplifier Design," Wiley, 1968.
4. Rohde, Ulrich L. and F. Hagemeyer, "Feedback Technique Improves Oscillator Phase Noise," *Microwaves & RF*, November 1998, pp. 61-70.
5. Hagemeyer, F., "Low Noise Oscillator Circuit Having Negative Feedback," US Patent 5,900,788, 4 May 1999.
6. Trask, C., "Distortion Improvement of Lossless Feedback Amplifiers Using Augmentation," *1999 IEEE Midwest Symposium on Circuits and Systems*, Las Cruces, New Mexico, August 1999.
7. Trask, C., "Lossless Feedback Amplifiers with Linearity Augmentation," US Patent 6,172,563, 9 January 2001.
8. Walls, F.L., E.S. Ferre-Pikal, and S.R. Jefferts, "The Origin of 1/f PM and AM Noise in Bipolar Junction Transistor Amplifiers," *1995 IEEE International Frequency Control Symposium* (IFCS 1995), pp. 294-304.
9. Darabi, H. and A.A. Abidi, "Noise in RF-CMOS Mixers: A Simple Physical Model," IEEE Transactions on Solid State Circuits, Vol. 35, No. 1, January 2000, pp. 15-25.
10. Bruccoleri, F., "Wide-Band Low-Noise Amplifier Techniques in CMOS," PhD dissertation, University of Twente, Enschede, The Netherlands, 2003.
11. Bruccoleri, F., A.M. Klumperink, and B. Nauta, "Wide-Band CMOC Low-Noise Amplifier Exploiting Thermal Noise Canceling," *IEEE Journal of Solid-State Circuits*, Vol. 39, No. 2, February 2004, pp. 275-282.
12. Bruccoleri, F., A.M. Klumperink, and B. Nauta, "Noise Canceling in Wideband CMOS LNAs," *2002 IEEE International Solid State Circuits Conferenece* (ISSCC 2002).
13. Bruccoleri, F., E.A.M. Klumperink, and B. Nauta, *Wideband Low Noise Amplifiers Exploiting Thermal Noise Cancellation*, Springer, 2005.
14. Chen, S.C., R.L. Wang, H.C. Kuo, M.L. Kung, and C.S. Gao, "The Design of Full-Band (3.1-10.6GHz) CMOS UWB Low Noise Amplifier with Thermal Noise Canceling," *2006 Asia-Pacific Microwave Conference*.
15. Im, D., I. Nam, H.T. Kim, and K. Lee, "A Wideband CMOS Low Noise Amplifier Employing Noise and IMS Cancellation for a Digital TV Tuner," IEEE Journal of Solid State Circuits, Vol. 44, No. 3, March 2009, pp. 686-698.
16. Li, Q., Y.P. Zhang, and J.S. Chang, "An Inductorless Low-Noise Amplifier with Noise Cancellation for UWB Receiver Front-End," 2006, pp.
17. Merkin, T.B., J.C. Li, S. Jung, M. Lu, J. Gao, and S.C. Lee, "A 100-960MHz CMOS Untra-Wideband Low Noise Amplifier," 2008, pp. 141-144.
18. Chin-Fu, L., C. Shih-Chien, and H. Po-Chiun, "A Noise-Suppressed Amplifier with a Signal-Nulled Feedback for Wideband Applications," *2008 IEEE Asian Solid-State Circuits Conference*, Fukuoka, Japan, November 2008.
19. Seader, L.D. and J.E. Sterrett, "Unit Transistor Amplifier with Matched Input and Output Impedances," US Patent 3,493,882, 3 February 1970.

20. Bode, H.W., *Network Analysis and Feedback Amplifier Design*, Van Nostrand, 1945.
21. Nordholt, E., "Classes and Properties of Multiloop Negative-Feedback Amplifiers," IEEE Transactions on Circuits and Systems, Vol. 28, No. 3, March 1981, pp. 203-211.
22. Nordholt, E.H., *Design of High-Performance. Negative-Feedback Amplifiers*, Elsevier, Amsterdam, 1983.
23. Trask, C., "Wideband Transformers: An Intuitive Approach to Models, Characterization and Design," *Applied Microwave & Wireless*, Vol. 13, No. 11, November 2001, pp. 30-41.
24. Lei, L., Z. Xiaodaan, L.G. Wang, and J. Minkyu, "Comparative Study and Analysis of Noise Reduction Techniques for Front-End Amplifiers," *2011 13th International Symposium on Integrated Circuits* (ISIC 2011), Singapore, December 2011.